Article

Not peer-reviewed version

Industrial Scale Direct Liquefaction of *Eucalyptus* Biomass

Irina Fernandes , José Condenço , Duarte Cecilio , Maria Joana Neiva Correia , João Carlos Moura Bordado , Margarida Mateus *

Posted Date: 8 August 2023

doi: 10.20944/preprints202308.0563.v1

Keywords: Energreen; Biomass liquefaction; Pilot Scale; Bio-oils; Sugars extraction; Stabilization

Article

Industrial Scale Direct Liquefaction of *Eucalyptus* Biomass

Irina Fernandes [2], José Condeço [2], Duarte M. Cecilio [1,2], Maria Joana Neiva Correia [2], João Bordado [2,3] and Margarida Mateus [1,2]*

[1] Secil S.A., Fábrica Secil – Outão, Setúbal, Portugal.
2 CERENA, Centro de Recursos Naturais e Ambiente, Departamento de Engenharia Química, Instituto Superior Técnico, Universidade de Lisboa, Lisboa, Portugal
* Correspondence: e-mail@e-mail.com; Tel.: (optional; include country code; if there are multiple corresponding authors, add author initials).

Abstract: This work presents the study of *Eucalyptus* bark and sawdust direct liquefaction. Laboratory scale experiments were carried out to assess the impact of several variables on the reaction yield and on the sugar content of the bio-oil. These variables were biomass type and concentration, the solvent and the reaction time. The results show that *Eucalyptus* sawdust presented the highest yields, but the highest sugar content after water extraction was obtained for *Eucalyptus* bark (~ 5.5% vs. 1.2% for sawdust). Simultaneously, industrial-scale tests were carried out at the ENERGREEN pilot plant using the same reaction variables, which resulted in reaction yields of nearly 100%. The reagents and raw materials used, as well as the products obtained (bio-oil, reaction condensates, polyols and sugar phases) were characterized by elemental analysis, infrared spectroscopy, thermogravimetry and high performance liquid chromatography with mass spectrometry. The heating value of the bio-oils is higher than that of the original biomass (higher heating value of *Eucalyptus* sawdust bio-oil 29 MJ/kg versus 19.5 MJ/kg of the original Eucalyptus sawdust). The analyses of the bio-oils allowed to identify the presence of high added-value compounds, such as levulinic acid and furfural. Finally, a study of the accelerated aging of the liquefied biomass showed that the biofuel density increases with the storage time due to the occurrence of repolymerization reactions.

Keywords: energreen; biomass liquefaction; pilot scale; bio-oils; sugars extraction; stabilization

1. Introduction

Fossil fuels are the largest source of energy currently in use due to its abundance and relative low cost. However, apart from being non-renewable sources of energy, fossil fuels have several negative environmental impacts, like global warming and air pollution. These negative impacts, together with the increase of the demand for energy sources, partially due to the huge increase of the world's population [1], have been the drivers for the increasing interest in renewable energy sources, namely biomass.

Biomass is considered the source of renewable energy with the greatest potential to bridge the energy needs of modern societies and includes forest residues (lignocellulosic biomass), industrial or domestic organic wastes [2,3]. From these, lignocellulosic biomass is one of most promising renewable energy resources, which can be used by direct combustion or by other efficient and competitive alternatives, such as thermochemical conversion, fermentation for bioethanol production or anaerobic digestion for biogas production [4].

Lignocellulosic biomass is formed by three main constituents: cellulose, hemicellulose and lignin [5,6]. Cellulose, with the molecular formula of $(C_6H_{10}O_5)_n$, is a linear polymer of glucose units connected through glycosidic bonds and can have crystalline or amorphous structure [7,8]. Crystalline cellulose is not depolymerizable at low temperatures [8,9]. Cellulose represents between 40-60% of the biomass composition. Hemicellulose, which constitutes between 20 to 40% of biomass, is an amorphous heteropolymer formed by monosaccharide units of hexoses, such as glucose, mannose and galactose, and pentoses, such as xylose and arabinose; hemicellulose chains are easily hydrolysed due to its branched structure and low molecular weight [6–8]. Finally, lignin, which can

represent between 10-25% of the biomass composition, is a highly branched amorphous biopolymer mainly composed of phenolic alcohols, such as p-coumaryl, synapil and conyferil alcohols; the high degree of branching of lignin leads to a three-dimensional network, which is difficult to chemically depolymerize [9].

There are a lot of publications about biomass direct liquefaction. Recently, the work of Fernandes *et al*.[10] describes the optimization of the liquefaction of *Eucalyptus* sawdust, namely the reaction time, catalyst concentration, temperature and the biomass-to-solvent ratio. The optimized conditions led to a maximum conversion rate of 96 %. Characterization of the bio-oil was performed using FTIR-ATR, elemental analysis and thermogravimetry. The characterization confirmed the presence of biomass-based compounds in the bio-oil. Paulo *et al*.[11] studied the acid-catalyzed liquefaction of eight short rotation coppice (SRC) poplar clones, aiming to convert the biomass into bio-oil at mild temperatures and ambient pressure. The produced bio-oil had a carbon content of 65%, oxygen content of 26% and hydrogen content of 8.7%, with an average higher heating value (HHV) of 30.5 MJ/kg. The van Krevelen diagram demonstrated that the bio-oils exhibited chemical compatibility with liquid fossil fuels like diesel or gasoline. The FTIR analysis indicated the substantial chemical conversion of the raw biomass, with evidence of the presence lignin and hemicellulose depolymerization derivatives in the bio-oil. TGA in nitrogen atmosphere showed that the bio-oils were more volatile than the fresh feedstock, requiring lower peaking temperatures for their vaporization and decomposition. Comparing the bio-oil with the biomass, the atomic ratios of H/C increase and O/C decrease, indicating that the bio-oil has better fuel characteristics. Overall, the liquefaction results confirmed the potential of SRC poplar biomasses for energy and chemicals production.

Silva et al.[12] quantified the sugars present in the aqueous extract of the bio-oil produced by thermochemical liquefaction of *Eucalyptus* globulus. The investigation employed HPLC-RID, a fast, economical and accurate analytical method, to identify and quantify the sugars in the aqueous extracts. HSQC-NMR and FTIR-ATR analyses confirmed the presence of carbohydrates in the aqueous extracts. The main sugars identified were fructose (36.58%), glucose (33.33%), sucrose (15.14%), trehalose (4.82%), and xylose (10.13%).

Liquefaction Process

Thermochemical conversion of biomass can be divided into three different processes: gasification, pyrolysis, and liquefaction. Liquefaction can be carried out in different conditions at high temperatures (>200 °C) and pressures, as in hydrothermal upgrading – HTU, or at moderated temperatures (100 – 250 °C) and atmospheric pressure in the presence of solvent and a catalyst, as in direct liquefaction studied in this work [4,13]. In this process, biomass chains are broken into smaller molecules by reaction with a solvent at temperatures between 150 to 250 °C and atmospheric pressure. Usually, a single or a mixture of polyhydric alcohols is used as solvent [14]. Biomass liquefaction is a significantly complex process due to the large variety of reactions that occur simultaneously, like the solvolysis between the biomass and the solvent, depolymerization of the major components of biomass, repolymerization, decarboxylation reactions, degradation reactions of oxygenated compounds in the presence of hydrogen, etc. [15,16]. The occurrence of several of these reactions is strongly influenced by the operating conditions (temperature, biomass type and composition, solvent, catalyst, etc.) [4,13]. From these, biomass composition and temperature are important variables. In fact, a low reaction temperature will lead to low liquefaction yields but high temperatures can lead to repolymerization reactions [16–18]. On the other hand, the relative composition in cellulose, hemicellulose and lignin greatly influences the behaviour of the biomass during liquefaction. In fact, the higher the amount of lignin the lower the conversion into bio-oil [4,18,19]. Actually, when lignin is thermally decomposed at high temperatures it forms free radicals of phenol that can react through re-polymerization and condensation reactions to produce solid residues [18]. Crystalline cellulose, with a more ordered structure, also presents low liquefaction rates [20].

Preprints (www.preprints.org) | NOT PEER-REVIEWED | Posted: 8 August 2023 doi:10.20944/preprints202308.0563.v1

In this work, the study of *Eucalyptus globulus* bark and sawdust biomass upgrading via direct liquefaction, carried out at laboratory and pilot scales, to yield a liquid biofuel with improved heating value and shelf life is presented.

2. Materials and Methods

2.1. Liquefaction

The biomass samples used in this work are Eucalyptus bark and Eucalyptus sawdust supplied by the Navigator Company. The optimum liquefaction conditions were studied elsewhere [Braz et al., 2019, Condeço et al., 2021]. Diethylene glycol (DEG) from Sapec, 2-Ethylhexanol (2EH) from Brenntag and the previously produced bio-oil were used as solvents; p-Toluenesulfonic acid was the catalyst. The liquefaction experiments described in this work were carried out at a laboratory scale, in a 2L batch reactor, and at a pilot scale in a 3 ton pilot reactor installed within the ENERGREEN project. Before all experiments, the biomass was pre-treated by contact with part of the solvent (typically ≈2 mL of solvent/100g of biomass at 80 °C for 60 minutes). In the pilot scale tests this pre-treatment is carried out inside the screw conveyor that transports the biomass to the reactor and this stage also takes around 60 min. This pre-treatment allows to promote the swelling of the cells allowing the better access of the catalyst to the biomass components [5].

Table 1. Experimental conditions used in the lab-scale liquefaction of Eucalyptus bark and Eucalyptus sawdust.

Conditions	*Eucalyptus* Bark	*Eucalyptus* Sawdust
Weight loss at 105ºC (%)	53.4	44.4
Ash (%)	5.1	1.7
Biomass (%)	10	10
Catalyst (%)	1.5	1.5
2EH (g)	750	750
Biomass (g)	188.3	152.4

Note: %- mass percentages.

The conditions used in the laboratory tests with Eucalyptus bark and sawdust are presented in ***Error! Reference source not found.***. To start each experiment, the solvent quantity was added to the reactor, the thermostat set to 80 °C and the stirrer was switched on and set at a speed of around 180 rpm. When the temperature reached 80 °C, the pre-treated biomass was added to the reactor and the thermostat was set at 160 °C. During the temperature rise, at around 99ºC, a mixture of water and solvent, which form an azeotrope (40% water and 60% solvent, w:w), was collected in a dean stark. After its complete removal, the temperature continues rising until the defined set point. When the reactor mixture reached 160 °C, the desired quantity of the catalyst was added to the reactor and the reaction timer was set to begin. After reaction, acetone was mixed with the reactor content and the mixture was filtered to separate the solids. The filtrate was distilled to remove the acetone and to recover the bio-oil. The solid residues were washed with acetone and dried at 80 °C in an oven and then cooled down to room temperature in a desiccator and weighted. The weight of residue was used to calculate the conversion of the biomass into bio-oil by using the following equation:

$$\%C = \frac{(W_i - W_f)}{W_i} \times 100 \quad (1)$$

where W_i and W_f are, respectively, the initial and final mass of solids.

In the laboratory tests carried out using sequential biomass additions, the solvent and the catalyst were added initially to the reactor and heated while stirring. When the reaction temperature

Preprints (www.preprints.org) | NOT PEER-REVIEWED | Posted: 8 August 2023 doi:10.20944/preprints202308.0563.v1

was reached, 10% wt of biomass vs. the solvent was added to the reactor. This procedure was repeated hourly until the limit condition, which corresponds to the formation of a very viscous mixture impossible to stir and filtrate.

The procedure used in the pilot reactor is described in EP1839810. Briefly, the biomass is transported to the reactor though a screw-conveyor where, as mentioned above, the solvent or the mixture of solvents is injected to promote the swelling of the biomass cells. Simultaneously, the preheating of the mixture is carried out through the counter-current passage of the vapours removed from the reactor. The liquefaction was carried out at atmospheric pressure and 160 °C. The biomass incrementation was 10% mass per hour.

The experimental conditions employed in the pilot-scale reactor were designed to replicate the conditions used in the laboratory experiments. Thus, Eucalyptus sawdust was selected as biomass and a concentration of 1.5% p-toluenesulfonic acid, relative to the amount of biomass, was used. In the first liquefaction reaction only 2EH was employed as solvent. However, in the subsequent two liquefaction reactions, a mixture of 2EH and DEG in a 1:1 mass ratio was utilized. In this pilot scale reactor the liquefaction process occurs in a semi-continuous mode according to the simplified flowsheet presented in ***Error! Reference source not found.***. After liquefaction the sugars produced by the decomposition of the lignocellulosic chains were extracted with water. After phases separation it was possible to obtain an aqueous phase, rich in several valuable compounds, and an organic phase, called polyols, that, after drying, is a valuable biofuel.

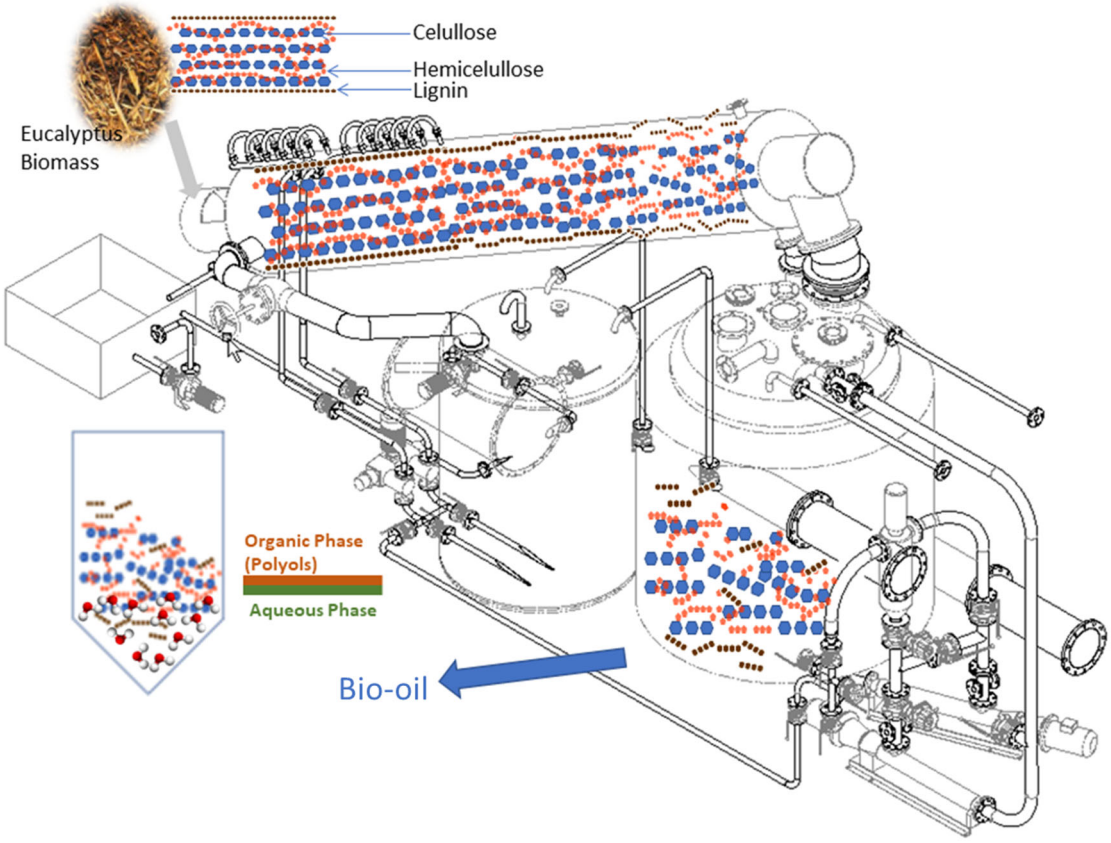

Figure 1. Flowsheet of the biomass liquefaction process and sugars extraction stage.

2.2. Sugars Extraction

In the laboratory tests the extraction of sugars from the bio-oils was carried out with distilled water or with the condensates recovered from the same liquefaction batch. After addition of the water/condensates in the proportion of 1:1 (weight) versus the bio-oil, the mixture was stirred slowly with a magnetic stirrer for 1 h and placed in a separating funnel overnight. After phases separation, the heavier yellowish aqueous phase is collected for analysis and the organic phase was weighed, dried and analyzed [12].

Preprints (www.preprints.org) | NOT PEER-REVIEWED | Posted: 8 August 2023 doi:10.20944/preprints202308.0563.v1

The aqueous phase after water extraction was further processed to determine its sugars content. Therefore, after vacuum filtration, a portion of the filtered solution is weighted and placed in an oven until constant weight. To avoid sugars degradation and caramelization during water evaporation, the oven was kept at 60°C. The sugar crystals were collected and weighted and the sugars content in the aqueous phase was determined using Equation (2, where the mass of water refers to the initial mass of water used in the extraction step.

$$Sugars\ content\ (\%) = \frac{Mass\ of\ Sugar\ crystals}{Mass\ of\ water} \times 100 \qquad (2)$$

2.3. Characterization Techniques

Several analytical techniques were used to characterize the biomasses and/or the liquefied products, namely thermogravimetric analysis (TGA- STA 449 F5 Jupiter equipment coupled with Proteus Analysis 6.1.0 software of NESTZSCH), elemental analysis and mid-infrared Fourier transformed spectroscopy (FTIR-ATR BOMEM FTLA2000-100, ABB CANADA in the 4000-400cm^{-1} range). TGA was used to determine the weight loss at
105 ºC of the bio-oils, whereas the water content of some of the samples was determined using the Karl-Fisher method. HPLC- MS (high-performance liquid chromatography with mass spectroscopy), which allows the analysis of polar compounds with high molecular weights, was also used. The system includes an Alliance 2695 HPLC chromatography unit and a Micromass Triple Quadrupole (Quattro Micro model) from Waters. The chromatography apparatus contains two columns in series: a pre-column XBridge BEH Amide 2.5 µm XP VanGuard Cartridge and a XBridge column BEH Amide 2.5 µm, both from Waters Corporation.

3. Results

3.1. Characterization of Biomass Feedstocks

The elemental composition and higher heating value (HHV) of the biomass samples are presented in Table 2. As seen, sawdust has a higher HHV and a lower moisture content, which will result in a lower energy consumption for water evaporation during liquefaction. It is also observed that the *Eucalyptus* bark has a higher ash content that will result in a higher content of solids after reaction.

Table 2. Biomass elemental composition (w:w) and heating values.

Biomass Analysis	*Eucalyptus* bark	*Eucalyptus* sawdust
Weight loss at 105ºC (%)	66.7	44.4
Ash (%)	6.4	1.7
C (%)*	46.0	49.3
H (%)*	5.3	5.7
N (%)*	1.2	1.0
S (%)*	0.1	0.1
Cl (%)*	0.2	0.1
O (%)**	47.2	43.8
HHV (kJ/kg)	17730	19460

daf- dry ash free basis; Oxygen determined by difference; mass percentages*

Preprints (www.preprints.org) | NOT PEER-REVIEWED | Posted: 8 August 2023 doi:10.20944/preprints202308.0563.v1

The FTIR spectra of the two biomass samples, together with the spectra of cellulose, hemicellulose and lignin standards, are presented in Figure 2.

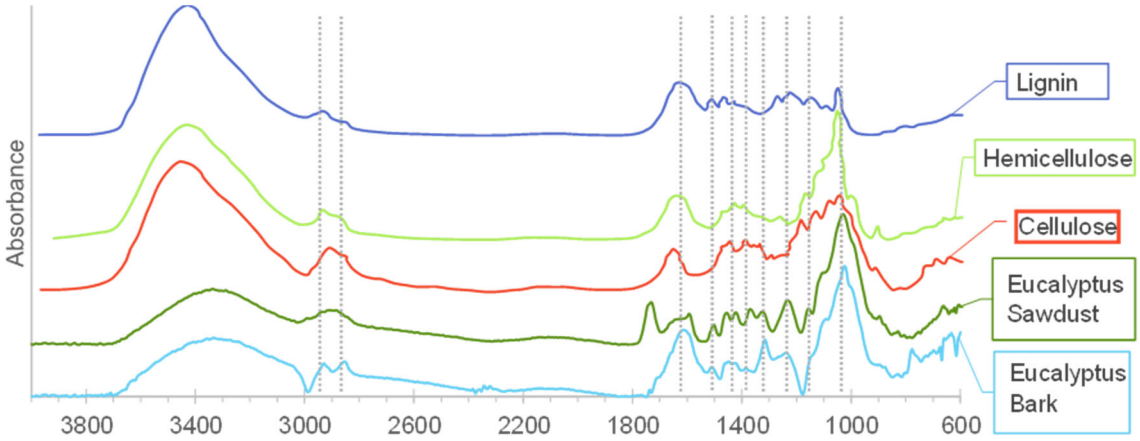

Figure 2. FTIR spectra of the biomasses and cellulose, hemicellulose and lignin standards.

By observing the FTIR spectra of the biomass samples and comparing them with the standard spectra of cellulose, hemicellulose, and lignin presented by Galletti et al. [21], it is possible to attribute the different peaks to each compound. Thus, the spectra of all samples display a prominent band within the range of 3500 - 3200 cm^{-1}, which can be attributed to the stretching vibration of hydroxyl groups. This intense signal in all biomasses indicates the presence of abundant hydroxyl functional groups due to, for example, moisture. *Eucalyptus* bark has peaks in the range of 2930 and 2850 cm^{-1} of aliphatic C–H stretching [14], characteristic of lignin and hemicellulose, whereas at these wavenumbers sawdust has a single peak also observed for cellulose. Another prominent peak in the spectrum of *Eucalyptus* bark and of the three biopolymers occurs at 1730-1620 cm^{-1} and is due to the C– O stretching of hemicellulose and lignin and to the C–C stretching of the lignin aromatic rings [14]. Peaks at 1510 cm^{-1} and 1320 cm^{-1} are found in the spectra of both biomasses and stand out, respectively, in the lignin and cellulose spectra. Finally, it is worth mentioning that the peak at 1025 cm^{-1} is seen in all spectra but with greater intensity in the spectrum of hemicellulose.

The TGA and DTG curves of the biomass samples and of the standards are presented in Figure 3. The TGA of *Eucalyptus* bark shows the first weight loss of 55.9% between 25 ºC and 140 ºC or, more precisely from the DTG curve, at 95.4 ºC. This mass loss is due to moisture evaporation. The second plateau, with a mass loss of 5.1%, occurs between 140-300 ºC; the comparison with the standards allows to conclude that this mass loss corresponds to the degradation of hemicellulose. The third plateau, corresponding to a mass loss of 20.0%, appears between 300 and 420 ºC, being the loss peak at 349.5 ºC, which corresponds to cellulose degradation. Finally, the fourth plateau, with a mass loss of 5.6%, is due to lignin degradation that occurs throughout the test. The solid residue determined by difference corresponds to 13.4%. It is worth noting that the results for *Eucalyptus* dust (not presented) were similar with some deviations on the pick temperatures.

Preprints (www.preprints.org) | NOT PEER-REVIEWED | Posted: 8 August 2023 doi:10.20944/preprints202308.0563.v1

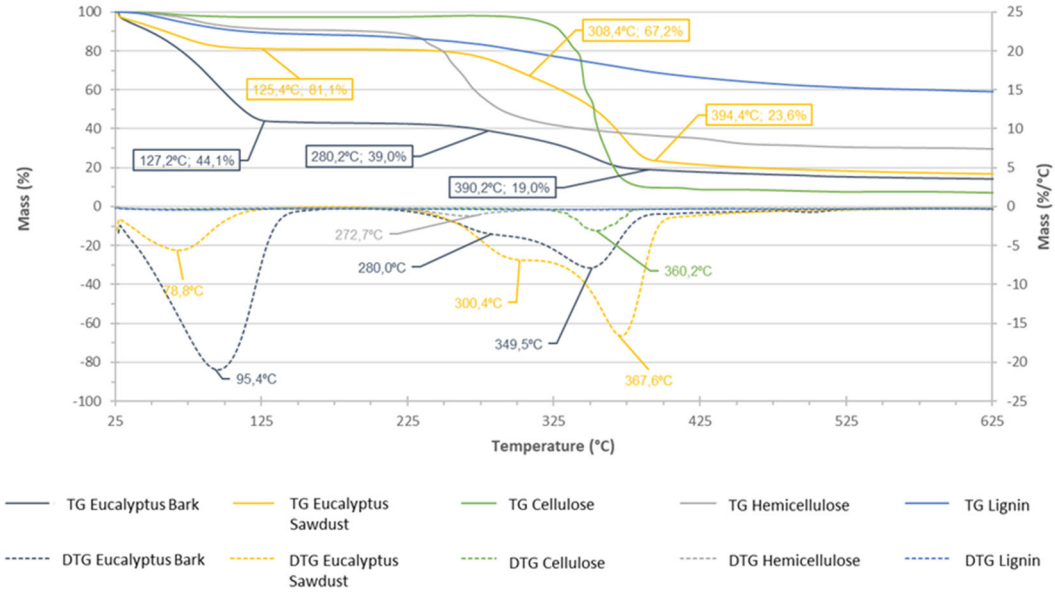

Figure 3. TGA (continuous line) and DTG (dotted line) analyses of the biomasses and standards.

The TGA results allowed to establish the relative composition (dry basis) in the three biopolymers of the two biomass samples (Table 3). As shown, *Eucalyptus* sawdust presents a higher content of hemicellulose and a lower content of lignin, which indicates that it should be easily liquified.

Table 3. Biomasses dry basis composition based on TGA (under N_2 atmosphere).

Composition	*Eucalyptus* Bark	*Eucalyptus* Sawdust
Hemicellulose	11.6%	17.1%
Cellulose	45.3%	53.8%
Lignin	12.7%	10.5%
Residue	30.4%	18.6%

3.2. Laboratory Scale Liquefaction

3.2.1. Semi Batch Liquefaction Tests

The *Eucalyptus* bark and sawdust liquefaction were performed in semi-batch mode using the conditions reported in Error! Reference source not found..

Biomass additions were made over time to mimic the industrial pilot-scale reaction. Error! Reference source not found. shows the observed decrease in the solvent mass percentage as biomass is introduced in the reactor, while the catalyst concentration remained between 2% and 3%.

Preprints (www.preprints.org) | NOT PEER-REVIEWED | Posted: 8 August 2023 doi:10.20944/preprints202308.0563.v1

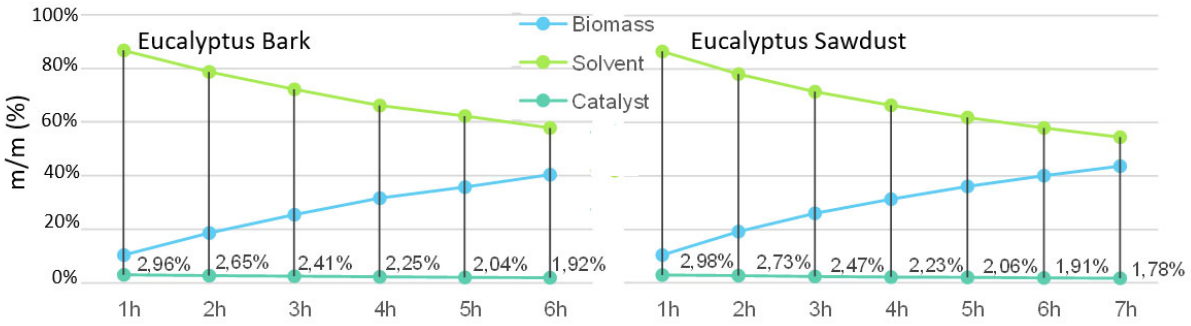

Figure 4. Biomass, solvent, and catalyst contents in the liquefaction of Eucalyptus bark and sawdust with sequential biomass additions.

It is worth noting that the reaction was stopped after 6 hours of bark addition and 7 hours of sawdust addition since the reaction medium became very viscous [22].

After liquefaction and sugars extraction with the reaction condensates, the drying of the aqueous phases at 60 ºC until constant weight allows to determine the sugars content. For bark, the mass of sugars recovered was 5.8% of the initial aqueous phase, whereas for sawdust this value was 1.2% [23].

The bio-oils and the hydrophobic fractions produced after sugars extraction, called polyols, were analysed. As seen in Error! Reference source not found., both phases have higher calorific values than the original biomasses (Table 2). Notably, the calorific value decreased from the liquefied product to the polyols phase, which can be attributed to the formation of a microemulsion with water during sugars extraction. In fact, the weight loss at 105 ºC verified for *Eucalyptus* bark polyols was 55.9%, higher than in the bio-oil. This increase was less pronounced for sawdust (6.8%) because the liquefied product already has a high-water content.

Table 4. Elemental analysis, weight loss at 105ºC and calorific values of the liquefied product and polyols of *Eucalyptus* bark and sawdust.

	***Eucalyptus* Bark**		***Eucalyptus* Sawdust**	
Analysis	**Bio-oil**	**Polyols**	**Bio-oil**	**Polyols**
Weight loss at 105 ºC (%)	7.0	62.9	46.8	53.6
C (%)*	62.4	45.2	65.3	56.3
H (%)*	11.7	9.3	9.7	9.8
N (%)*	1.8	1.2	1.3	1.2
S (%)*	0.3	0.1	0.4	0.3
O (%)**	23.8	44.2	23.3	32.4
HHV (kJ/kg)	32915	21585	32405	27685

*daf- dry ash free basis;** Oxygen determined by difference; mass %.

FTIR spectra of samples of the liquefied product taken before each addition of *Eucalyptus* bark to the reactor were also collected. As shown in Error! Reference source not found., all liquefied products exhibited the characteristic peaks of 2EH spectrum. On the other hand, the peaks at 1750 cm^{-1} and 1235 cm^{-1} increased in intensity with the number of biomass increments. These peaks correspond to C=O bonds, characteristic of ketone or aldehyde functional groups, and COOH bonds, characteristic of carboxylic groups [12,24]. The increase in these peaks intensity with the reaction time can be attributed to cellulose depolymerization into levulinic acid and furfural, or to an increase in

Preprints (www.preprints.org) | NOT PEER-REVIEWED | Posted: 8 August 2023 doi:10.20944/preprints202308.0563.v1

hemicellulose content due to the addition of biomass [23,25,26]. The elongated peak in the range of 3300 cm^{-1}, representing OH groups, is typically associated with moisture [24].

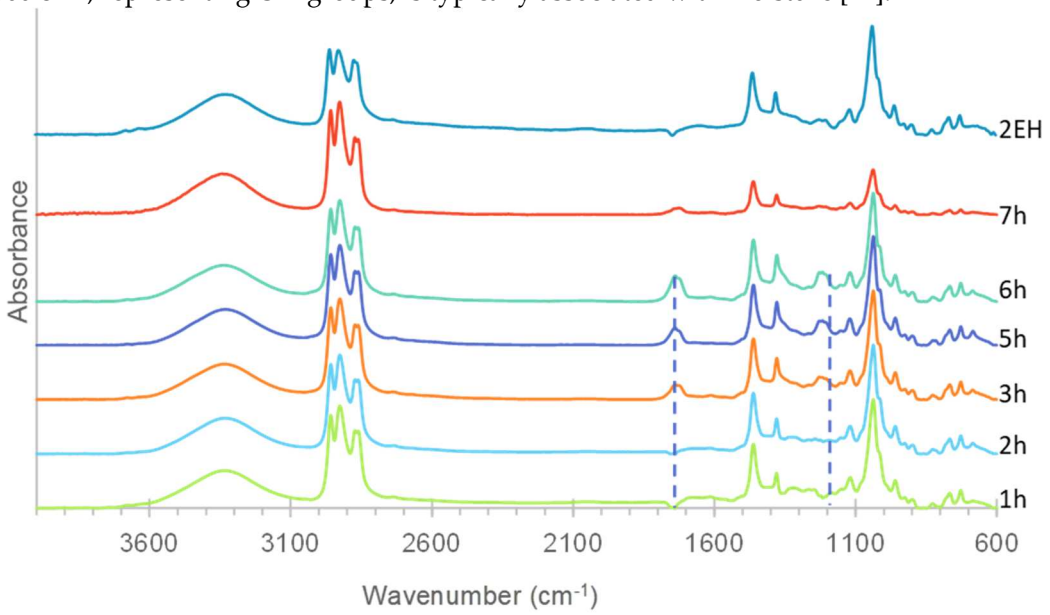

Figure 5. FTIR spectra of the liquefied product before each incremental addition of *Eucalyptus* bark.

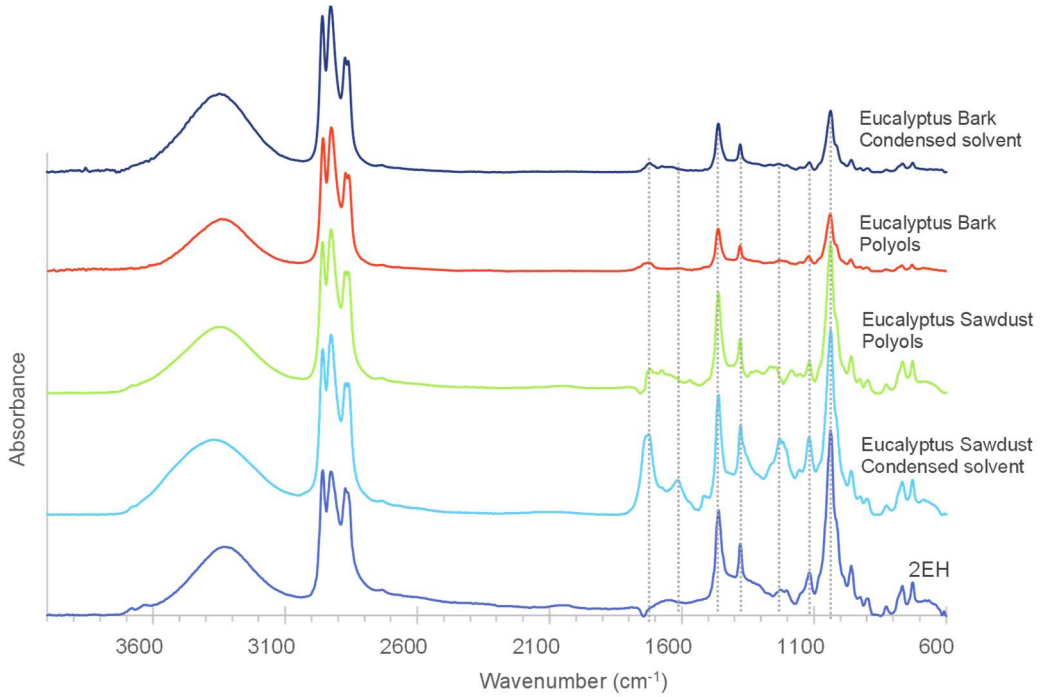

displays the FTIR spectra of polyols and of pure and condensed solvent. As seen, the polyols exhibit peaks corresponding to 2EH, particularly in the 3000-2800 cm^{-1} range. The peaks at 1790 cm^{-1} and 1685 cm^{-1} in the polyols spectrum are characteristic of C=O bonds [22]. These peaks indicate the presence of soluble fragments produced during the depolymerization reactions, such as levulinic acid, lactic acid and/or furfural [25,26]. However, these peaks can also be attributed to the presence of partially depolymerized hemicellulose and lignin [24]. The band at 1610 cm^{-1}, due to CH_2 bonds, can also indicate the presence of cellulose and hemicellulose polymers [12]. Finally, the peaks at 1575, 1465, 1213, 1138, 877 and 839 cm^{-1} are observed in the spectra of pure and condensed solvent.

Preprints (www.preprints.org) | NOT PEER-REVIEWED | Posted: 8 August 2023 doi:10.20944/preprints202308.0563.v1

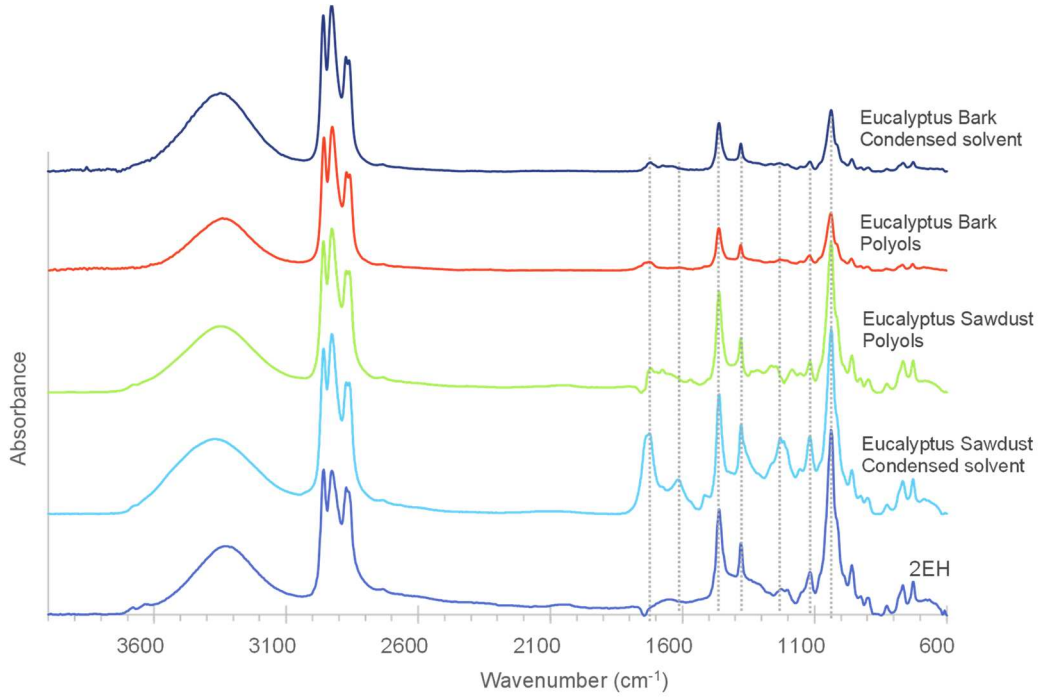

Figure 6. FTIR spectra of the polyols and pure and condensed solvent from the liquefaction reaction of *Eucalyptus* bark and sawdust.

3.3. Pilot Scale Liquefaction Tests

In addition to the laboratory experiments, several tests were conducted in an industrial liquefaction pilot facility using the laboratory-established conditions. The main objective of the ENERGREEN pilot plant is to produce a clean and sustainable biofuel with a high calorific value to be used in the cement kiln. Therefore, the reaction products obtained after liquefaction of *Eucalyptus* sawdust, namely the liquefied biomass, the polyols, the condensates, the extraction waters and the sugars resulting from the reactions were analyzed using the previously described techniques.

3.3.1. Characterization of the Bio-Oils

Table 5 presents the elemental analysis, calorific value, density and viscosity of the bio-oil produced in *Eucalyptus* sawdust liquefaction.

Table 5. Elemental analysis, weight loss at 105 ºC, calorific value and density of bio-oils produced in the 1st liquefaction reaction (Solvent: 2EH).

Reaction Time (h)	**24h**	**48h**
Weight loss at 105ºC %(m/m)	-	40.0
C (%)*	70.3	44.1
H (%)*	12.9	11.1
N (%)*	2.3	1.1
S (%)*	0.3	0.9
O (%)**	14.2	42.8
HHV (kJ/kg)	38790	22880
LHV (kJ/kg)	36065	20525
Density (kg/dm^3)	0.80 (25ºC)	0.92 (25ºC)

Preprints (www.preprints.org) | NOT PEER-REVIEWED | Posted: 8 August 2023 doi:10.20944/preprints202308.0563.v1

*daf- dry ash free basis; ** Oxygen determined by difference; %-mass percentage.

The results presented in Error! Reference source not found. reveal a slight increase in density with time and with biomass additions. Regarding the calorific value of the liquefaction products, it is found that it is higher than that of the initial biomass (HHV=19530 kJ/kg), indicating that the bio-oil is of higher value. The high value of the weight loss at 105ºC after 48h of reaction (40%) is certainly correlated with 2EH-water azeotrope. Nevertheless, the average water content, determined by the Karl Fisher method, of the liquefied samples at the end of the reaction was only 2.1%.

Previous work showed that the best liquefaction conversion was obtained when a mixture 1:1 of DEG and 2-EH was used as solvent [4]. Therefore, two tests were carried out using this mixture of solvents (Table 6 and 7)

Table 6. Elemental analysis, weight loss at 105 ºC, moisture content, calorific value and density of the liquefied product produced in the 2nd liquefaction reaction. (Solvent: 2EH and DEG 1:1).

Reaction Time (h)	24	48	56	96	120
Weight loss at 105ºC %	-	59.8	-	28.1	
Moisture (%)					9.2
C (%)*	58.5	49.9	57.4	55.4	61.9
H (%)*	9.6	10.1	9.9	9.0	8.6
N (%)*	1.2	-	-	1.3	1.3
S (%)*	0.7	0.3	0.5	0.7	0.9
O (%)**	30.0	39.8	32.2	33.6	27.3
HHV (kJ/kg)	28595	24374	28200	26780	29730
LHV (kJ/kg)	26565	-	26110	24870	27950
Density (kg/dm³)	-	-	1.02 (25ºC)	-	1.41 (25ºC)

*daf- dry ash free basis;** Oxygen determined by difference; mass percentages.

Table 7. Elemental analysis, weight loss at 105 ºC, moisture content, calorific value and density of the liquefied product produced in the 3rd reaction. (Solvents: 2EH and DEG).

Reaction Time (h)	4	8	12	24	48	56
Weight loss at 105ºC %(m/m)	35.1	35.7	35.1	35.2	31.9	35.9
Moisture %(m/m)						2.1
C (%)*	62.6	62.9	62.4	62.2	60.4	60.8
H (%)*	9.0	9.1	9.5	9.4	9.0	9.3
S (%)*	0.8	0.8	0.7	0.6	0.8	0.7
O (%)**	27.6	27.2	27.5	27.8	29.9	29.3
HHV (kJ/kg)	30282	30364	30551	29933	28530	29108
Density (kg/dm³)	1.36	1.37	1,33	1.36	1.39	1.40

*daf- dry ash free basis;** Oxygen determined by difference; mass percentages

Comparing the values presented in Tables 5 to 7, it is possible to conclude that the bio-oils produced in these three liquefactions were similar. Furthermore, since DEG is denser and more

Preprints (www.preprints.org) | NOT PEER-REVIEWED | Posted: 8 August 2023 doi:10.20944/preprints202308.0563.v1

viscous than 2EH, the density of the liquefied products obtained using the mixture of solvents is higher than when EH was used alone. Again, the high weight loss at 105 ºC of the different samples in Table 7 is also due to the 2EH-water azeotrope. However, as shown in Table 6 and 7, the water content of the bio-oils was only 9.2% and 2.1 %, respectively.

FTIR Analysis

The FTIR spectra of the bio-oils produced in different stages of the 1st pilot liquefaction are presented in Error! Reference source not found., alongside the spectra of the solvent and catalyst. As seen, the presence of 2EH in the liquefied products is revealed by the peaks at 2958, 2926, 2872, 1460, 1380, and 1038 cm^{-1}. On the other hand, the intensity of the band at around 1730 cm^{-1} increases with the reaction time. As mentioned above, this band corresponds to the presence of carboxylic groups and can be associated with compounds derived from depolymerization reactions, such as lactic acid, levulinic acid or furfural [27,28]. Nevertheless, this peak may also indicate the presence of unreacted biomass since biomass is continuously added to the reactor. The peaks at 1590 and 1170 cm^{-1} in the bio-oil spectra are associated with the catalyst and correspond to C=C bonds of the aromatic rings and to R-SO2-OH bonds. Thus, it is possible to conclude that the catalyst was not entirely removed. The peak at 1590 cm^{-1} may also be associated with aromatic vibrations of lignin polymers with C=O bonds. Finally, the low-intensity peaks at 766 and 726 cm^{-1} in the solvent spectrum corresponds to C-C bond vibrations.

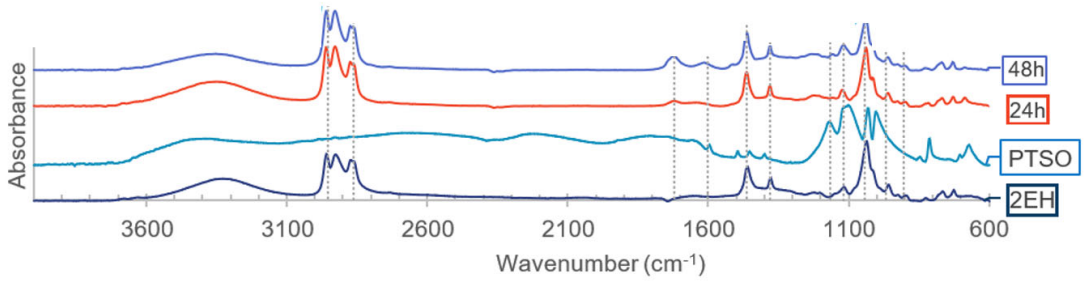

Figure 7. FTIR analysis of 2-EH, catalyst and of 1st liquefaction bio-oils (solvent: 2EH).

The spectrum of the bio-oils produced in one of the reactions carried out with the mixture of 2EH and DEG as solvent is presented in Error! Reference source not found. (reaction 3 in Supporting Information) and shows that the bio-oils and polyols contain 2EH and DEG. In fact, the peaks at 2958, 2926, and 2872 cm^{-1} due to C-H bonds are visible in both phases. On the other hand, the peak at 1350 cm^{-1}, representing C-OH vibrations, as well as at 1215 and 1118 cm^{-1}, associated with C-O bonds of esters, and the peaks at 912 and 886 cm^{-1}, corresponding to C-O-C bonds, indicates the presence of DEG. The peak at 1038 cm^{-1}, indicative of C-OH groups of both solvents, appears in the spectra of all samples.

The analysis of the FTIR spectra of the bio-oils and polyols samples reveals a peak at 1640 cm^{-1}, corresponding to C=C bonds of furfural or HMF (hydroxymethylfurfural), which result from the depolymerization reactions of cellulose and lignin [25,27]. This peak is present in the spectra of bio-oils and polyols, showing that these species were not completely extracted to the aqueous phase.

Preprints (www.preprints.org) | NOT PEER-REVIEWED | Posted: 8 August 2023 doi:10.20944/preprints202308.0563.v1

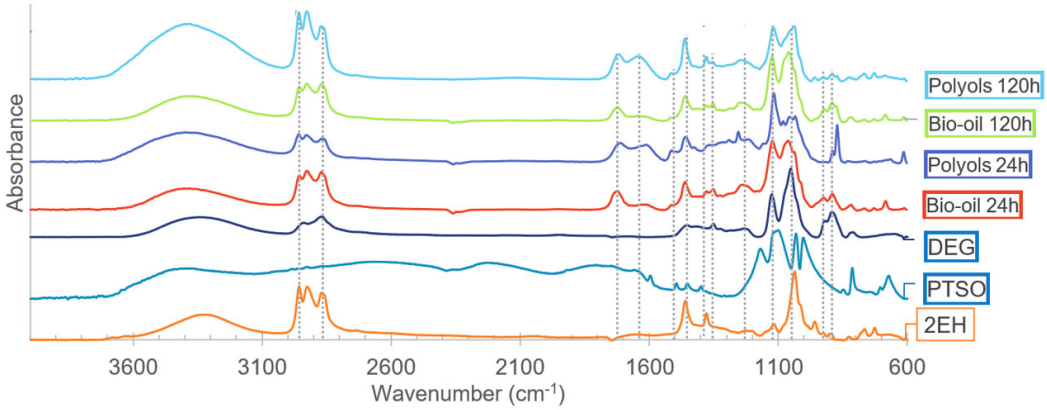

Figure 8. FTIR analysis of the solvents, catalyst, bio-oils and polyols produced in the 3rd liquefaction reaction (solvent: 2EH and DEG).

TG/DTG/DSC Analysis

Error! Reference source not found. presents the thermogravimetric analysis of the bio-oil produced after 56 h of the 2nd liquefaction reaction.

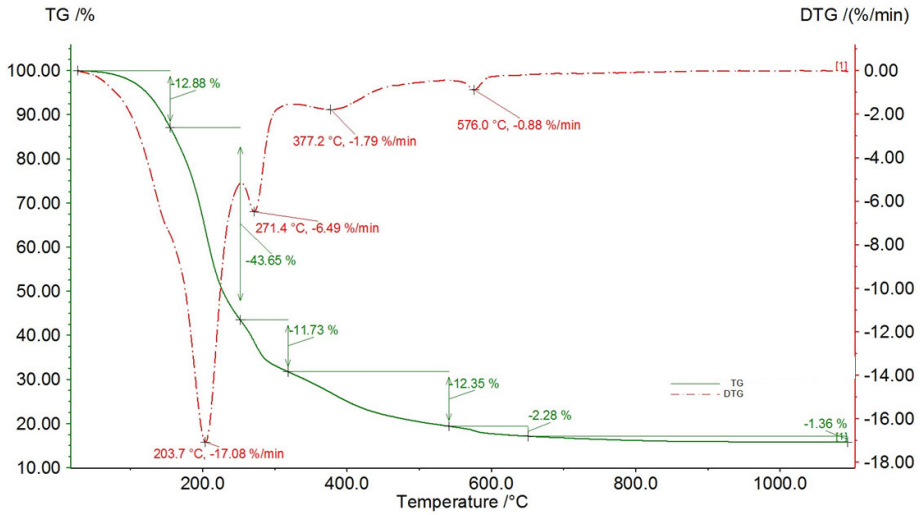

Figure 9. TG/DSC/DTG curves of the bio-oil produced after 56h of the 2nd liquefaction reaction (solvent: 2EH and DEG).

The DTG curve above shows an initial slope variation at 139.0°C, indicating a significant mass loss of 12.9% until 207°C. The 207-286°C temperature interval exhibits the highest mass rate variation of approximately 45.1%, peaking at 251.4°C, suggesting that the compounds within this temperature range are the most abundant in the liquefied product. Beyond 286°C, the mass loss rate decreases significantly, with a further loss of 15.6% until 353°C. The DTG curve stabilizes at this point, indicating a constant mass variation with time. The decomposition observed in this range may be attributed to the degradation of non-reacted biomass constituents, particularly lignin polymers. Lastly, a minor peak weight loss is observed at 581.9°C, which could be associated with the degradation of more complex compounds that either did not decompose during the reaction or resulted from repolymerization reactions.

The TG curve of the 8 h product from the third reaction shown in Error! Reference source not found. exhibits a distinct pattern. In fact, five distinct plateaus in the TG and DTG curves can be

 doi:10.20944/preprints202308.0563.v1

distinguished: the first plateau spans from 25 to 152°C, with a mass loss of 12.9%; the second plateau, ranging from 152 to 253°C, includes the most pronounced peak of mass loss at 204°C, resulting in a loss of 43.7% of the sample mass. This temperature range corresponds to the degradation of DEG. The third plateau (253-295°C) peaks at 271.4°C, indicating a further 9.7% mass loss. The last two plateaus occur between 295-466°C and 466-603°C, with 12.4% and 2.3% mass losses, respectively.

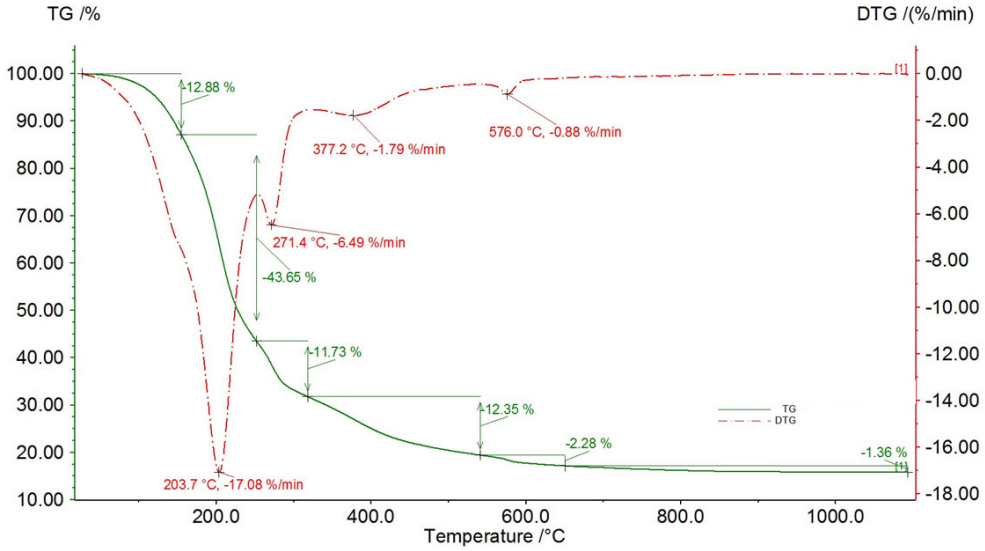

Figure 10. TG/DSC/DTG curves for an 8h sample of 3rd liquefaction reaction (solvent: 2EH and DEG).

3.3.2. Characterization of the Aqueous Phases and Dried Sugars

FTIR Analysis

The FTIR analysis of the aqueous phases obtained in the water extractions of the bio-oils produced in the 2nd liquefaction after 56h and 120h of reaction is presented in Figure 11. As seen, both samples exhibit an elongated band at approximately 3400 cm^{-1}, corresponding to moisture [29]. The peaks at 2959, 2929, and 2873 cm^{-1} are associated with C-H bonds, characteristic of the solvent 2EH. Similar peaks in the range of 1462 and 1379 cm^{-1} are also related to C-H vibrations. The prominent peaks at 1121, 1056, 926, and 890 cm^{-1}, representing C-O bonds, C-OH vibrations, and C-O-C bonds of ester groups, match with the peaks of DEG, which is highly soluble in water.

Figure 11 also shows that are several peaks in the spectra of the aqueous phases that do not belong to the solvents. Notably, the peak at 1648 cm^{-1} observed in the FTIR spectrum of the extraction water collected after 56h of reaction corresponds to vibrations associated of the C=C bonds. Furthermore, two additional peaks were recorded at frequencies of 1723 and 1235 cm^{-1}, which can be attributed to carboxylic groups and COOH vibrations, respectively. Thus, through comparison with reference spectra of different sugars, it was concluded that the above-mentioned peaks are also present in the spectra of furfural, HMF (hydroxymethylfurfural), lactic acid and levulinic acid.

Preprints (www.preprints.org) | NOT PEER-REVIEWED | Posted: 8 August 2023 doi:10.20944/preprints202308.0563.v1

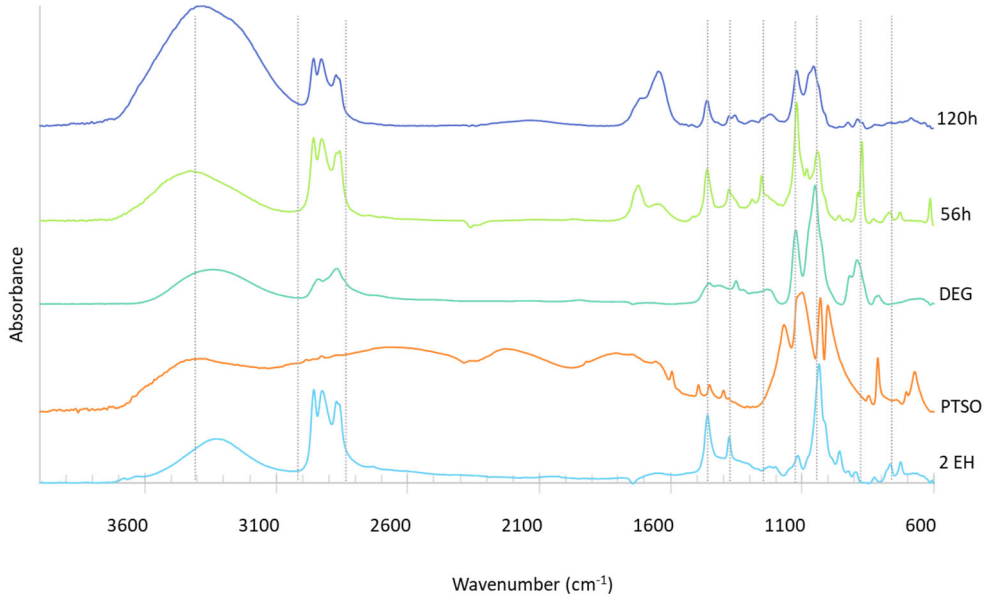

Figure 11. FTIR Analysis of extraction waters of the 2nd liquefaction reaction (solvent: 2EH and DEG).

presents the FTIR spectra of the dried sugars solutions recovered from the aqueous phases of water extraction of two bio-oils (24h and 48h) of the 1st liquefaction reaction. The spectra exhibit bands of the catalyst, specifically at 1102, 1032, 1005, 814, and 673 cm^{-1} of R-SO2-OH, O=S=O, S-C, and S-O bonds. Therefore, it is possible to conclude that the catalyst is transferred to the aqueous phase during the extraction process, a hypothesis further corroborated by the acidic pH of the extraction waters (1.7 in this case). Additionally, the spectra have a band in the region of 3300 cm^{-1}, indicating the presence of hydroxyl (-OH) groups associated with either moisture or alcohol. As expected, the intensity of this band decreases as the drying temperature increases from 60°C to 80°C.

In the sugars sample recovered from the 24h reaction bio-oil, two peaks at 2931 and 2874 cm^{-1} are evident. These peaks correspond to aliphatic compounds containing carbon-hydrogen bonds. On the other hand, in the sugars dried at 60°C, prominent peaks appear at frequencies of 1720 and 1651cm^{-1}, which can be attributed to carbonyl and conjugated double bonds, respectively.

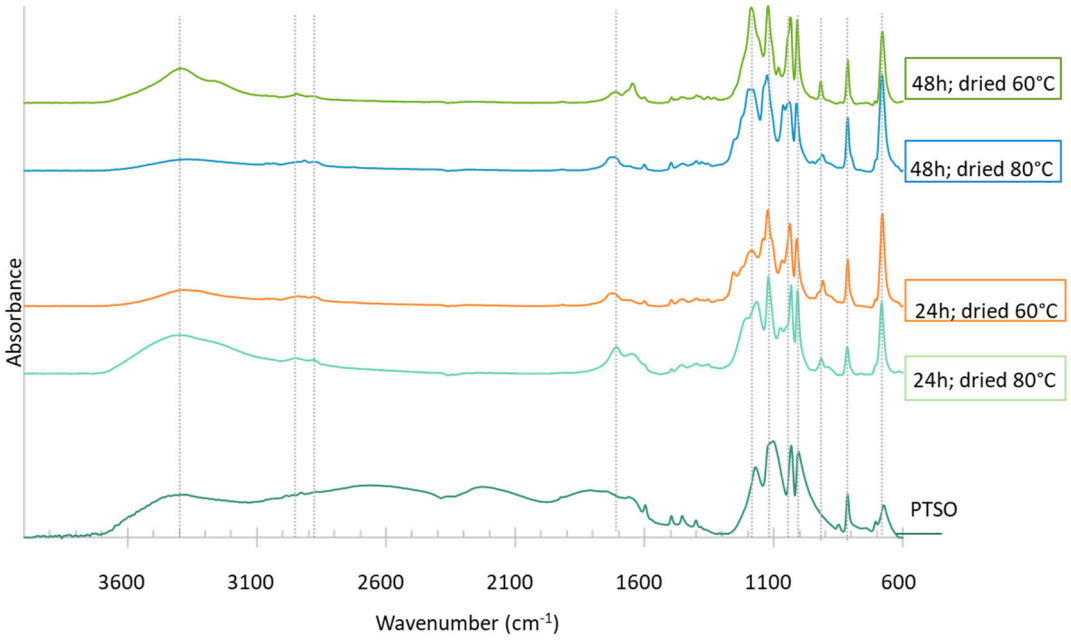

Preprints (www.preprints.org) | NOT PEER-REVIEWED | Posted: 8 August 2023 doi:10.20944/preprints202308.0563.v1

Figure 12. FTIR analysis of dried sugars extracted from bio-oils produced in the 1st liquefaction after 24h and 48h of reaction (solvent: 2EH).

TG/DTG/DSC Analysis

Thermogravimetry analysis was also used to analyse the aqueous phases of bio-oils water extraction (Figure 13) and some of the sugars recovered after drying of these aqueous phases (Figure 14 and 15).

In the DTG curve of the extraction water in Figure 13, three peaks are observed at 150.2, 196.9 and 245.7°C, whereas in the dried sugars resulting from this water (Figure 14), three peaks also appear but at different temperatures of 183.7, 259.7, and 479.4°C. Probably, the first peaks in each curve, at 150.2 and 183.7°C, may correspond to the same compound. In fact, the mass loss associated with water in the aqueous phase has a huge influence on this DTG curve, overlapping with the peak at 183.7°C. After water removal, the concentration of this component increases, showing a peak at 100°C with an associated mass loss of 13.49%. The analysis of the DTG curves of several pure compounds that can be present in these aqueous phases (supplementary information) shows that furfural has a decomposition temperature close to 172.1°C, similar to the temperature at which the mass loss of the analyzed sugars occurs. Although there is still a considerable difference in these peak temperatures, the color and odor of the obtained sugar solutions resemble those described for furfural, which is a yellowish liquid with a strong odor [30].

Another peak that appears in the three TG/DTG curves is the mass loss peak at around 245°C. Comparison with DTG curves of standard compounds (supplementary information) allows to conclude that this peak is characteristic of both levulinic acid and lactic acid, which confirms the findings of the FTIR spectra that indicate the presence of the functional groups of these compounds.

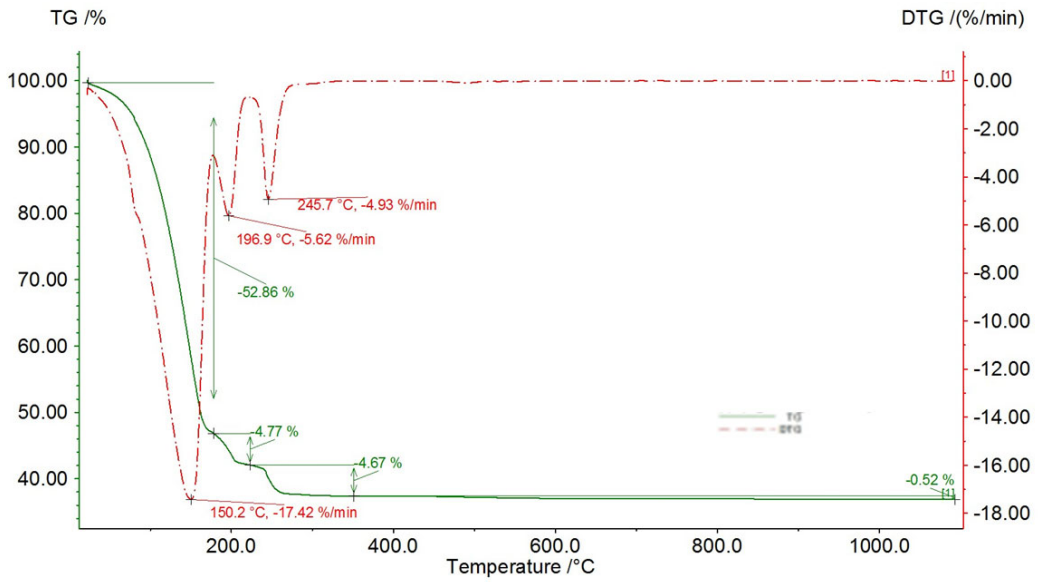

Figure 13. TG/DSC/DTG curves of the aqueous phase after water extraction of the bio-oil produced in the 1st liquefaction after 24h of reaction (solvent: 2EH).

Preprints (www.preprints.org) | NOT PEER-REVIEWED | Posted: 8 August 2023 doi:10.20944/preprints202308.0563.v1

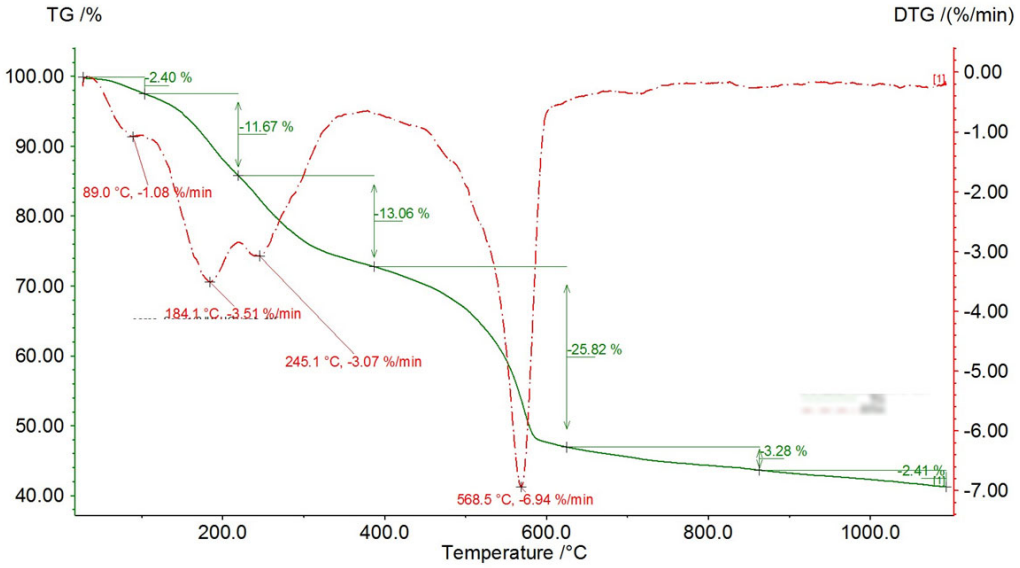

Figure 14. TG/DSC/DTG curves of the dried sugars recovered from the aqueous phase of water extraction of the bio-oil produced in the 1st liquefaction after 24h of reaction (solvent: 2EH).

In addition to the previously mentioned peak at 180°C (5.0% mass loss), the sugars exhibit a peak in the range of 240-250°C (62.7% mass loss), identified as either lactic acid or levulinic acid. This sample also has distinctive mass loss peaks, particularly at 320.5 and 581.7°C, with mass variations of 16.1% and 2.0%, respectively. The peak at 320°C is characteristic of glucose (supplementary information), which is also found in sugar dimers such as cellobiose formed by two glucose molecules.

HPLC-MS/MS Analysis

HPLC MS/MS was the analytical technique used to characterise the sugars in the aqueous phase produced in bio-oils water extraction. First, the relevant standard solutions presented in Table 8 were individually injected in the mass spectrometry instrument to identify their characteristic fragmentation patterns. The collision energy was adjusted for each molecule under investigation. During the infusion process, the first quadrupole was set to the molecular mass of the corresponding standard ion, and the specific fragmentations of each identified signal (resulting from bond cleavage of lower mass ions) were determined by analyzing the molecular masses and the chemical structures after collision with argon in the collision cell. This procedure allowed to identify the specific transitions for each standard that is essential for the HPLC analysis. The observed fragmentations were attributed to various processes including the loss of H_2O, formation of double bonds, loss of -CH_2O groups, loss of H_2, or cleavage of bonds within aromatic rings [31–34].

Table 8. Standards used in the HPLC-MS/MS.

Standards	
Arabinose Xylose Ribose	Succinic Acid
Glucose Sorbose Galactose Frutose	Levulinic Acid

Mannose	
Lactic Acid	Xylitol
Cellobiose Trehalose	Rhamnose

The comparison between the standards retention times with the ones of the injected solutions allowed to identify the main compounds in solution. However, some of the standards with identical masses that were grouped in the mass spectrometry analysis, have different retention times in the HPLC run (Supplementary Information). Nevertheless, this HPLS-MS/MS analysis revealed the presence of intense peaks of levulinic acid and of the catalyst (PTSO) (supplementary materials). These findings are consistent with the results obtained from FTIR analysis.

3.3.3. Characterization of the Reaction Condensates

The condensates recovered during the liquefaction reactions are expected to be formed by a mixture of the solvent/s with the water from the biomass moisture and formed during the depolymerization reactions.

FTIR Analysis of the Condensates

The FTIR spectra of the organic and aqueous phases obtained after phases separation of the condensates collected after 24 and 48h of reaction in the 3rd liquefaction are presented in Figure 15, together with the spectra of the pure solvents and of lactic acid.

As seen, the spectra of the aqueous and organic phases present the same peaks. Furthermore, the peaks characteristic of 2EH (2960, 2929, 2873, 1462, 1121, 1035, 826, 768, and 729 cm^{-1}) and DEG (1215, 1121, 1035, 961, and 892 cm^{-1}) are present in the condensates, which confirms that part of the solvents are carried over during water evaporation. Additionally, the peaks at 1731, 1235, 1178, and 1117 cm^{-1}, corresponding to C=O bonds, -COOH groups, C-O bond vibrations, and C-OH vibrations, respectively, attributed to carboxylic acid functional groups are also present in the condensates but not in the solvents. The comparison with the spectra of different compounds, it was observed that these peaks can be due to the presence of lactic acid in the condensates, which was also carried away from the reaction medium during evaporation.

The peaks at around 3374 cm^{-1}, corresponding to OH groups, is very important in the aqueous phase of the condensates of the 48h reaction sample. Furthermore, the peak at 1640 cm^{-1}, typically associated with C=C vibrations, is also present and can be attributed to the presence of furfural and HMF.

Preprints (www.preprints.org) | NOT PEER-REVIEWED | Posted: 8 August 2023 doi:10.20944/preprints202308.0563.v1

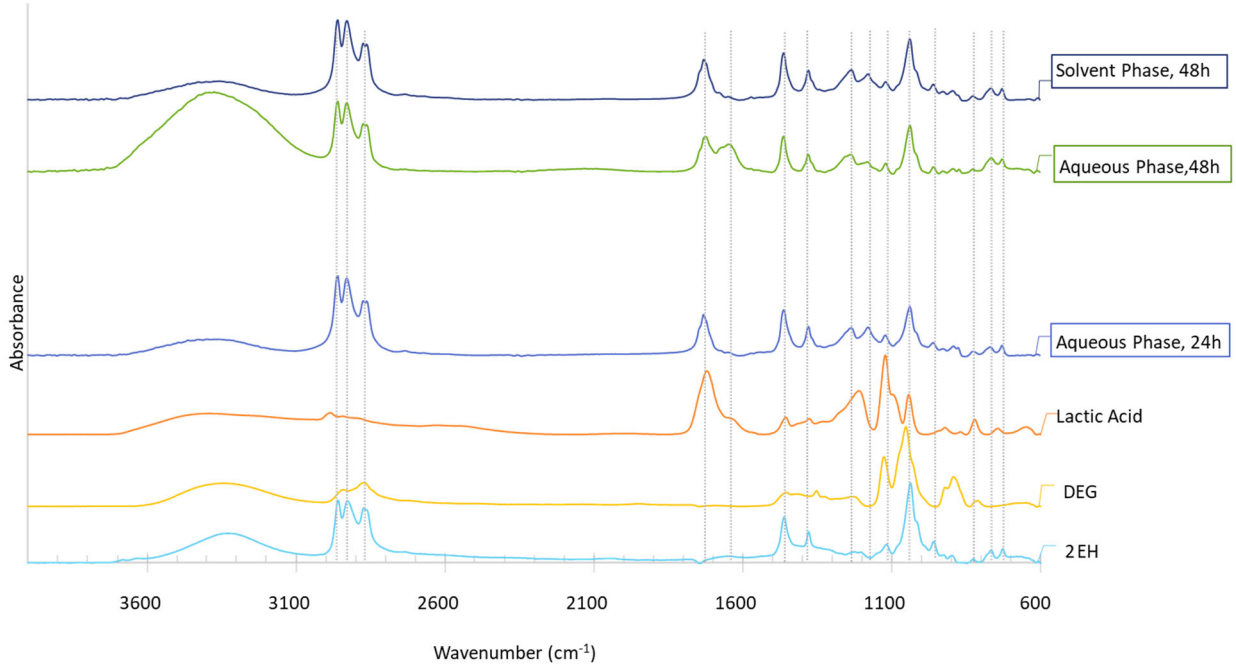

Figure 15. FTIR spectrum of 3rd liquefaction condensates.

Having in mind the previous results, it is possible to conclude that the evaporation of the water, produced by the depolymerization reactions and by biomass dehumidification, carries some solvent. Moreover, the acidic pH of the condensed aqueous phase can be due to the presence of carboxylic acids and/or some catalyst. Finally, the FTIR spectra of the condensates aqueous phases indicate that some of the products of the depolymerization reactions, like lactic acid, levulinic acid and furfural, are also removed from the reaction medium to the condensates.

3.3.4. Bio-Oil Ageing

One factor that can hinder the widespread use of biofuels in industrial applications is their tendency to degrade over time during storage. To study the effect of the storage time on the properties of these bio-oils, a sample of the bio-oil produced in the 3rd liquefaction after 10 hours of reaction was used. The aging process was accelerated by subjecting the biofuel sample to a temperature of 80ºC, following the method described by Udomsap et al. [35].

Therefore, three bio-oil samples were put in an oven at 80 ºC for 1, 2, and 7 days. After the specified aging period, the samples were removed from the oven and cooled. The density was measured after cooling, and it was not possible to measure the viscosity because the samples were solid at room temperature.

It is worth noting that according to Oasmaa et al., the changes observed after 24 hours at 80 ºC are equivalent to the changes that would occur if the biofuel is kept at room temperature for one year [36]

The density measurements of the fresh and aged bio-oils are presented in Figure 16. As expected, the density of the bio-oils increases with the storage time [37] following a linear relation (R^2=0.99). This density increase can be attributed to the occurrence of repolymerization reactions due to the presence of free radicals in the biofuel. These radical reactions form compounds with larger molecular weight, thereby increasing the overall density of the biofuel.

Preprints (www.preprints.org) | NOT PEER-REVIEWED | Posted: 8 August 2023 doi:10.20944/preprints202308.0563.v1

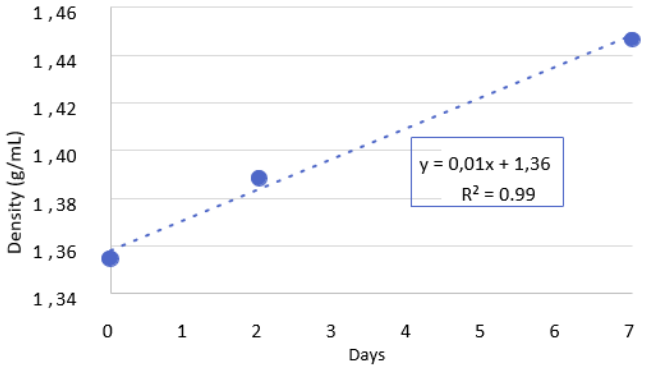

Figure 16. Evolution of bio-oil density with time (3rd reaction, 10h).

One of the alternatives to minimize biofuel degradation during storage is the addition of a solvent that can easily undergo dehydrogenation reactions, as the released hydrogen atoms will react rapidly with the free radicals, thus hindering the repolymerization reactions responsible for bio-oil degradation [38].

5. Conclusions

This work presents a comparative study of the use of *Eucalyptus* sawdust and bark as biomass feedstock for biofuel production. TG analysis allowed to conclude that *Eucalyptus* bark undergoes significant weight loss at specified temperatures due to moisture evaporation and biopolymers degradation. Sawdust displayed a similar trend, albeit with minor variations in peak temperatures. Based on these findings, the comparative composition of the two biomasses established from the TG analysis anticipates an easier liquefaction of sawdust owing to its higher hemicellulose and lower lignin contents.

In the laboratory-scale liquefaction experiments of bark and sawdust, a highly viscous liquid was produced after 6 or 7 incremental additions of biomass, respectively. The drying at 60 ºC of the aqueous phases obtained after extraction of the sugars contained in bio-oils with the reaction condensates allowed to recover a mass of sugars of 5.8% of the initial aqueous phase for bark, whereas for sawdust this value was only 1.2%. Interestingly, bio-oils and polyols have higher calorific values than the original biomasses. However, a decrease was observed from bark bio-oil to the polyols, likely due to the formation of a water microemulsion during sugars extraction.

The FTIR spectra of the bio-oils produced in various liquefaction stages revealed the presence of compounds derived from biomass depolymerization, such as lactic acid, levulinic acid and furfural. The presence of unreacted biomass and of the catalyst was also detected. Additionally, the comparison with the TGA degradation profiles of bio-oils and several standards helped to identify the presence of several biomass degradation products in the bio-oils.

HPLC-MS/MS analysis validated the presence of levulinic acid and the catalyst (PTSO) in the aqueous phase obtained in bio-oils water extraction. The characterization of reaction condensates via FTIR analysis identified the presence of the solvent/s and of lactic acid that are carryover during water evaporation from the reactor. The acidic pH of the condensates suggested the presence of carboxylic acids and/or some catalyst.

Finally, the study on bio-oil aging showed an increase in bio-oil density with the storage time, which can be attributed to repolymerization reactions mediated by free radicals. Therefore, it is possible to conclude that storage conditions and duration significantly influence the properties and quality of the biofuel.

In conclusion, the results obtained in this work allow to conclude that *Eucalyptus* sawdust is a promising feedstock for sustainable biofuel production and biorefinery.

6. Patents

EP18398010 - Ângela Nunes, João Bordado, Joana Neiva Correia, Margarida Mateus, Flávio Oliveira, Rui Lopes, Catalytic and continuous thermochemical process of production of valuable derivatives from organic materials and waste, 2018.

Supplementary Materials: The following supporting information can be downloaded at: www.mdpi.com/xxx/s1

Author Contributions: For research articles with several authors, a short paragraph specifying their individual contributions must be provided. The following statements should be used "Conceptualization, X.X. and Y.Y.; methodology, X.X.; software, X.X.; validation, X.X., Y.Y. and Z.Z.; formal analysis, X.X.; investigation, X.X.; resources, X.X.; data curation, X.X.; writing—original draft preparation, X.X.; writing—review and editing, X.X.; visualization, X.X.; supervision, X.X.; project administration, X.X.; funding acquisition, Y.Y. All authors have read and agreed to the published version of the manuscript." Please turn to the CRediT taxonomy for the term explanation. Authorship must be limited to those who have contributed substantially to the work reported.

Acknowledgments: In this section, you can acknowledge any support given which is not covered by the author contribution or funding sections. This may include administrative and technical support, or donations in kind (e.g., materials used for experiments).

Conflicts of Interest: The authors declare no conflict of interest.

References

1. IEA *Global Energy & CO2 Status Report 2019*; IEA: Paris, 2019;
2. McKendry, P. Energy Production from Biomass (Part 2): Conversion Technologies. *Bioresour. Technol.* **2002**, *83*, 47–54, doi:10.1016/S0960-8524(01)00119-5.
3. Bridgwater, T. Biomass for Energy. *J. Sci. Food Agric.* **2006**, *86*, 1755–1768, doi:10.1002/jsfa.2605.
4. Braz, A.; Mateus, M.M.; Santos, R.G. dos; Machado, R.; Bordado, J.M.; Correia, M.J.N. Modelling of Pine Wood Sawdust Thermochemical Liquefaction. *Biomass Bioenergy* **2019**, *120*, 200–210, doi:10.1016/j.biombioe.2018.11.001.
5. Aysu, T.; Küçük, M.M. Biomass Pyrolysis in a Fixed-Bed Reactor: Effects of Pyrolysis Parameters on Product Yields and Characterization of Products. *Energy* **2014**, *64*, 1002–1025, doi:10.1016/j.energy.2013.11.053.
6. González-García, P. Activated Carbon from Lignocellulosics Precursors: A Review of the Synthesis Methods, Characterization Techniques and Applications. *Renew. Sustain. Energy Rev.* **2018**, *82*, 1393–1414, doi:10.1016/j.rser.2017.04.117.
7. Zhang, L.; Xu, C. (Charles); Champagne, P. Overview of Recent Advances in Thermo-Chemical Conversion of Biomass. *Energy Convers. Manag.* **2010**, *51*, 969–982, doi:https://doi.org/10.1016/j.enconman.2009.11.038.
8. Xu, F.; Yu, J.; Tesso, T.; Dowell, F.; Wang, D. Qualitative and Quantitative Analysis of Lignocellulosic Biomass Using Infrared Techniques: A Mini-Review. *Appl. Energy* **2013**, *104*, 801–809, doi:10.1016/j.apenergy.2012.12.019.
9. Cecílio, D.M.; Gonçalves, J.R.M.; Correia, M.J.N.; Mateus, M.M. Aspen Plus® Modeling and Simulation of an Industrial Biomass Direct Liquefaction Process. *Fuels* **2023**, *4*, 221–242, doi:10.3390/fuels4020014.
10. Fernandes, F.; Matos, S.; Gaspar, D.; Silva, L.; Paulo, I.; Vieira, S.; C. R. Pinto, P.; Bordado, J.; Galhano dos Santos, R. Boosting the Higher Heating Value of Eucalyptus Globulus via Thermochemical Liquefaction. *Sustainability* **2021**, *13*, 3717, doi:10.3390/su13073717.
11. Paulo, I.; Costa, L.; Rodrigues, A.; Orišková, S.; Matos, S.; Gonçalves, D.; Gonçalves, A.R.; Silva, L.; Vieira, S.; Bordado, J.C.. Acid-Catalyzed Liquefaction of Biomasses from Poplar Clones for Short Rotation Coppice Cultivations. *Molecules* **2022**, *27*, 304, doi:10.3390/molecules27010304.
12. Silva, L.; Orišková, S.; Gonçalves, D.; Paulo, I.; Condeço, J.; Monteiro, M.; Xavier, N.M.; Rauter, A.P.; Bordado, J.M.; Galhano dos Santos, R. Quantification of Hydrolytic Sugars from Eucalyptus Globulus Bio-Oil Aqueous Solution after Thermochemical Liquefaction. *Forests* **2023**, *14*, 799, doi:10.3390/f14040799.
13. Pan, H. Synthesis of Polymers from Organic Solvent Liquefied Biomass: A Review. *Renew. Sustain. Energy Rev.* **2011**, *15*, 3454–3463, doi:10.1016/J.RSER.2011.05.002.
14. Condeço, J.A.D.; Hariharakrishnan, S.; Ofili, O.M.; Mateus, M.M.; Bordado, J.M.; Correia, M.J.N. Energetic Valorisation of Agricultural Residues by Solvent-Based Liquefaction. *Biomass Bioenergy* **2021**, *147*, 106003, doi:10.1016/j.biombioe.2021.106003.
15. Behrendt, F.; Neubauer, Y.; Oevermann, M.; Wilmes, B.; Zobel, N. Direct Liquefaction of Biomass. *Chem. Eng. Technol.* **2008**, *31*, 667–677, doi:10.1002/ceat.200800077.

16. Lu, Y.; Li, G.-S.; Lu, Y.-C.; Fan, X.; Wei, X.-Y. Analytical Strategies Involved in the Detailed Componential Characterization of Biooil Produced from Lignocellulosic Biomass. *Int. J. Anal. Chem.* **2017**, *2017*, e9298523, doi:10.1155/2017/9298523.
17. Jiang, W.; Kumar, A.; Adamopoulos, S. Liquefaction of Lignocellulosic Materials and Its Applications in Wood Adhesives—A Review. *Ind. Crops Prod.* **2018**, *124*, 325–342, doi:10.1016/J.INDCROP.2018.07.053.
18. Zhong, C.; Wei, X. A Comparative Experimental Study on the Liquefaction of Wood. *Energy* **2004**, *29*, 1731–1741, doi:10.1016/J.ENERGY.2004.03.096.
19. Zhang, W.; Liu, H.; Ul Hai, I.; Neubauer, Y.; Schröder, P.; Oldenburg, H.; Seilkopf, A.; Kölling, A. Gas Cleaning Strategies for Biomass Gasification Product Gas. *Int. J. Low-Carbon Technol.* **2012**, *7*, 69–74, doi:10.1093/ijlct/ctr046.
20. Li, Y.; Luo, X.; Hu, S. Lignocellulosic Biomass-Based Polyols for Polyurethane Applications. In *Bio-based Polyols and Polyurethanes*; Li, Y., Luo, X., Hu, S., Eds.; SpringerBriefs in Molecular Science; Springer International Publishing: Cham, 2015; pp. 45–64 ISBN 978-3-319-21539-6.
21. Raspolli Galletti, A.M.; D'Alessio, A.; Licursi, D.; Antonetti, C.; Valentini, G.; Galia, A.; Nassi o Di Nasso, N. Midinfrared FT-IR as a Tool for Monitoring Herbaceous Biomass Composition and Its Conversion to Furfural. *J. Spectrosc.* **2015**, *2015*, e719042, doi:10.1155/2015/719042.
22. Amândio, M.S.T.; Rocha, J.M.S.; Xavier, A.M.R.B. Enzymatic Hydrolysis Strategies for Cellulosic Sugars Production to Obtain Bioethanol from Eucalyptus Globulus Bark. *Fermentation* **2023**, *9*, 241, doi:10.3390/fermentation9030241.
23. Liu, Y.; Shi, H.; Wang, Y.; Wen, J. Analysis of Chemical Components and Liquefaction Process of Eucalyptus Globulus Bark. *Appl. Chem. Eng.* **2021**, *4*, 29–36, doi:10.24294/ace.v4i2.1347.
24. Fernandes, A.; Cruz-Lopes, L.; Dulyanska, Y.; Domingos, I.; Ferreira, J.; Evtuguin, D.; Esteves, B. Eco Valorization of Eucalyptus Globulus Bark and Branches through Liquefaction. *Appl. Sci.* **2022**, *12*, 3775, doi:10.3390/app12083775.
25. Knez, Ž.; Hrnčič, M.K.; Čolnik, M.; Škerget, M. Chemicals and Value Added Compounds from Biomass Using Sub- and Supercritical Water. *J. Supercrit. Fluids* **2018**, *133*, 591–602, doi:10.1016/j.supflu.2017.08.011.
26. De Bhowmick, G.; Sarmah, A.K.; Sen, R. Lignocellulosic Biorefinery as a Model for Sustainable Development of Biofuels and Value Added Products. *Bioresour. Technol.* **2018**, *247*, 1144–1154, doi:10.1016/j.biortech.2017.09.163.
27. Zhou, C.-H.; Xia, X.; Lin, C.-X.; Tong, D.-S.; Beltramini, J. Catalytic Conversion of Lignocellulosic Biomass to Fine Chemicals and Fuels. *Chem. Soc. Rev.* **2011**, *40*, 5588–5617, doi:10.1039/C1CS15124J.
28. Grilc, M.; Likozar, B.; Levec, J. Hydrotreatment of Solvolytically Liquefied Lignocellulosic Biomass over NiMo/Al2O3 Catalyst: Reaction Mechanism, Hydrodeoxygenation Kinetics and Mass Transfer Model Based on FTIR. *Biomass Bioenergy* **2014**, *63*, 300–312, doi:10.1016/j.biombioe.2014.02.014.
29. Water Absorption Spectrum Available online: https://water.lsbu.ac.uk/water/water_vibrational_spectrum.html (accessed on 14 July 2023).
30. ICSC 0276 - FURFURAL Available online: http://www.ilo.org/dyn/icsc/showcard.display?p_version=2&p_card_id=0276 (accessed on 14 July 2023).
31. Demarque, D.P.; Crotti, A.E.M.; Vessecchi, R.; Lopes, J.L.C.; Lopes, N.P. Fragmentation Reactions Using Electrospray Ionization Mass Spectrometry: An Important Tool for the Structural Elucidation and Characterization of Synthetic and Natural Products. *Nat. Prod. Rep.* **2016**, *33*, 432–455, doi:10.1039/C5NP00073D.
32. Taylor, V.F.; March, R.E.; Longerich, H.P.; Stadey, C.J. A Mass Spectrometric Study of Glucose, Sucrose, and Fructose Using an Inductively Coupled Plasma and Electrospray Ionization. *Int. J. Mass Spectrom.* **2005**, *243*, 71–84, doi:10.1016/j.ijms.2005.01.001.
33. Konda, C. Structural Analysis of Carbohydrates by Mass Spectrometry. PhD, University of Purdue, 2013.
34. Haider Shipar, Md.A. Formation of Methyl Glyoxal in Dihydroxyacetone and Glycine Maillard Reaction: A Computational Study. *Food Chem.* **2006**, *98*, 395–402, doi:10.1016/j.foodchem.2005.03.042.
35. Udomsap, P.; Yeinn, Y.H.; Hui, J.T.H.; Yoosuk, B.; Yusuf, S.B.; Sukkasi, S. Towards Stabilization of Bio-Oil by Addition of Antioxidants and Solvents, and Emulsification with Conventional Hydrocarbon Fuels. In Proceedings of the 2011 International Conference & Utility Exhibition on Power and Energy Systems: Issues and Prospects for Asia (ICUE); September 2011; pp. 1–5.
36. Oasmaa, A.; Kuoppala, E. Fast Pyrolysis of Forestry Residue. 3. Storage Stability of Liquid Fuel. *Energy Fuels* **2003**, *17*, 1075–1084, doi:10.1021/ef030011o.
37. Adjaye, J.D.; Sharma, R.K.; Bakhshi, N.N. Characterization and Stability Analysis of Wood-Derived Bio-Oil. *Fuel Process. Technol.* **1992**, *31*, 241–256, doi:10.1016/0378-3820(92)90023-J.
38. Zhang, S.; Yang, X.; Zhang, H.; Chu, C.; Zheng, K.; Ju, M.; Liu, L. Liquefaction of Biomass and Upgrading of Bio-Oil: A Review. Molecules 2019, 24, 2250. https://doi.org/10.3390/molecules24122250

 doi:10.20944/preprints202308.0563.v1